Chemistry
A European
Journal

Chemistry Europe
European Chemical Societies Publishing

Accepted Article

Title: Electron storage capability and singlet oxygen productivity of a Ru(II) photosensitizer containing a fused naphthaloylenebenzene moiety at the 1,10-phenanthroline ligand

Authors: Yingya Yang, Jannik Brückmann, Wolfgang Frey, Sven Rau, Michael Karnahl, and Stefanie Tschierlei

To be cited as: *Chem. Eur. J.* 10.1002/chem.202001564

Link to VoR: https://doi.org/10.1002/chem.202001564

WILEY-VCH

10.1002/chem.202001564

WILEY-VCH

FULL PAPER

Electron storage capability and singlet oxygen productivity of a Ru(II) photosensitizer containing a fused naphthaloylenebenzene moiety at the 1,10-phenanthroline ligand

Yingya Yang,[a,‡] Jannik Brückmann,[a,‡] Wolfgang Frey,[b] Sven Rau,[a] Michael Karnahl,*[,b] and Stefanie Tschierlei*[,a]

Abstract: As a novel rylene type dye a diimine ligand with a fully rigid and extended π-system in its backbone was prepared by directly fusing a 1,10-phenanthroline building block with 1,8-naphthalimide. The corresponding heteroleptic ruthenium photosensitizer bearing one biipo and two tbbpy ligands was synthesized and extensively analyzed by a combination of NMR, single crystal X-ray diffraction, steady-state absorption and emission, time-resolved spectroscopy and different electrochemical measurements supported by time-dependent density functional theory calculations. The cyclic and differential pulse voltammograms revealed, that the naphthaloylene-benzene moiety enables an additional second reduction of the ligand. Moreover, this ligand possesses a very broad absorption in the visible region. In the Ru(II) complex this causes an overlap of ligand-centered and metal-to-ligand charge transfer transitions. The emission of the complex is clearly redshifted compared to the ligand emission with very long-lived excited states lifetimes of 1.7 and 24.7 µs in oxygen-free acetonitrile solution. This behavior is accompanied by a surprisingly high oxygen sensitivity. Finally, this photosensitizer was successfully applied for the effective evolution of singlet oxygen challenging some of the common Ru(II) prototype complexes.

Introduction

The capture, storage and usage of solar light for light-driven reactions in organic synthesis[1-4] and for the production of solar fuels[5-8] or singlet oxygen ($^1O_2$) is of strongly increasing importance.[9-12] As $^1O_2$ is one of the most relevant reactive oxygen species (ROS) for photodynamic therapy (PDT), there is a great need for effective singlet oxygen generating chromophores.[13-16] This requires the design of efficient and stable photosensitizers with suitable redox potentials and excited state lifetimes. Moreover, for some applications (*e.g.* the reduction of protons to hydrogen) photosensitizers are desired that are able to store multiple charges.[17-22] In this context especially Ru(II) polypyridine complexes containing an additional electron storage moiety at the diimine ligand have been extensively studied.[17,19,20,23,24] For instance, different types and number of methyl viologen, anthraquinone, naphthalimide or pyrene derivatives had been introduced as an additional substituent to 2,2'-bipyridine (bpy) or 1,10-phenanthroline (phen).[23-27,28]

The integration of donor-acceptor units like naphthalene dicarboxylic acid monoimide (NMI) or other rylene derivatives enabled easy synthetic access to photosensitizers with high thermal and (photo)chemical stabilities and to adapt the photophysical as well as electrochemical properties of the chromophores in a wide range. In addition, rylene dyes often provide high fluorescence quantum yields, large extinction coefficients over a broad spectral range and the option to store multiple electrons.[29-35] The usage of related dyes like naphthalene tetracarboxylic acid bisbenzimidazole (perinone) allows for low energy gaps and light absorption over a wide range.[36-38] However, due to their low solubility, these ligand systems received only limited attention.[36-38]

In contrast to the extension of the π-system of the diimine ligand by different substituents, the main aim of this study was the direct integration of a naphthaloylenebenzene unit in the backbone of the 1,10-phenanthroline ligand (Figure 1) to obtain a fully conjugated and rigid ligand. It is expected that this modification not only affects the redox behavior, but also the charge transfer processes and efficiency. To this end, 16H-benzo[4',5']isoquinolino[2',1':1,2]imidazo[4,5-f]-[1,10]-phenanthrolin-16-one (**biipo**) and its heteroleptic Ru(II) complex $[(tbbpy)_2Ru(biipo)]^{2+}$ (**Rubiipo**, with tbbpy = 4,4'-*tert*.-butyl-2,2'-bipyridine) were prepared and analyzed (including single crystal X-ray diffraction (XRD)) for the first time (Figure 1). Cyclic and differential pulse voltammetry were used to evaluate the effect of the internal electron storage on the redox chemistry. A combination of steady-state and time-resolved emission spectroscopy along with transient absorption spectroscopy and (time-dependent) density functional theory (TD-)DFT calculations were then used to explore the photophysical properties and charge-transfer processes. Moreover, **Rubiipo** was successfully used for the evolution of $^1O_2$ competing some of the parent standard complexes like $[Ru(bpy)_3]^{2+}$ (**Rubpy**) or $[(tbbpy)_2Ru(phen)]^{2+}$ (**Ruphen**).

[a] Y. Yang, J. Brückmann, Prof. Dr. S. Rau, Dr. S. Tschierlei
Ulm University, Institute of Inorganic Chemistry I
Albert-Einstein-Allee 11, 89081 Ulm, Germany.
E-mail: stefanie.tschierlei@uni-ulm.de.

[b] Dr. W. Frey, Dr. M. Karnahl
University of Stuttgart, Institute of Organic Chemistry
Pfaffenwaldring 55, 70569 Stuttgart, Germany.
E-mail: michael.karnahl@oc.uni-stuttgart.de

‡ Both authors contributed equally to this work.

Supporting information for this article is given via a link at the end of the document. The supporting information (SI) includes experimental and synthetic information, crystallographic data, NMR, MS and UV/vis spectra, cyclic voltammograms as well as results of the (TD-)DFT calculations.

10.1002/chem.202001564

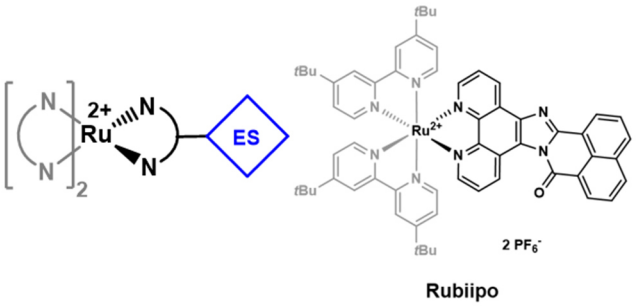

Figure 1. Schematic representation of a Ru(II) photosensitizer containing an additional electron storage (ES) moiety (left) and the structure of **Rubiipo** investigated in this study (right). The **biipo** ligand is depicted in black.

Results and Discussion

Synthesis and structural characterization

The synthesis of the **biipo** ligand was performed via a four-step procedure (Scheme S2.1) starting from 1,10-phenanthroline. In the final step 5,6-diamino-1,10-phenanthroline and a slight excess of 1,8-naphthalic anhydride were condensed to yield **biipo** as a yellow solid in 94 % (Figure 2). Subsequently, due to its low solubility **biipo** was coordinated to the $[(tbbpy)_2RuCl_2]$ precursor using hot ethylene glycol as solvent. This procedure is also applied for similar poorly soluble diimine ligands and is known in literature.[39,40] **Rubiipo** was then purified *via* silica column chromatography (for further details see SI) and counter ion exchange to obtain the complex in a total yield of 71 %.

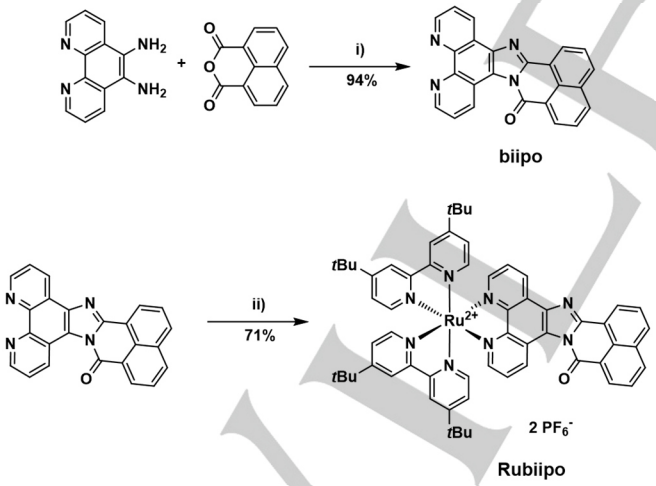

Figure 2. Preparation of the **biipo** ligand and its corresponding Ru(II) complex **Rubiipo**. Conditions: i) acetic acid, Ar, 140°C, 24 h and ii) $[(tbbpy)_2RuCl_2]$, ethylene glycol, 120°C, 20 h.

Rubiipo was fully characterized by ^1H and ^{13}C nuclear magnetic resonance (NMR) spectroscopy, high-resolution mass spectrometry (HRMS, electron spray ionization), IR spectroscopy, elemental analysis and single crystal XRD (see all spectra in the SI). **Rubiipo** and **biipo** both exhibit a characteristic carbonyl stretch vibration at around 1700 cm^{-1} in their IR spectra (Figures S3.15 and S3.16) originating from the **biipo** ligand framework. The high-resolution mass spectra of both the ligand and the complex match very well with theoretical data and simulated isotopic patterns (see Figures S3.9 and S3.10). In the ^1H NMR spectra the chemical shifts of all aromatic protons appear as expected.[41,42] The proton signals of the two bipyridines, the phenanthroline and the naphthaloylene-benzene moiety suggest an asymmetric octahedral Ru(II) complex. Moreover, the aliphatic protons of the tertiary butyl (*t*Bu) groups show a small splitting (*i.e.* four separated singlet signals with 9 protons each), which is caused by the asymmetric structure of the **biipo** ligand. Caused by this asymmetry the four pyridines and *t*Bu groups of the two tbbpy ligands are not equivalent within the **Rubiipo** complex and possess a different chemical environment. Further, ^1H NMR spectra with different concentrations of **Rubiipo** (in the range from 1.28 mM to 32.1 mM, Figure S3.6) exhibit considerable shifts of the proton signals of up to 0.5 ppm. According to literature protocols, a dimerization constant of 27 M^{-1} was determined for **Rubiipo** (see SI).[43-46] This clearly suggests intermolecular interactions between different **Rubiipo** species in solution, which are caused by the quite large and planar **biipo** ligand. This observation is in line with other Ru(II) complexes bearing polycyclic diimine ligands such as dipyridophenazine, tetrapyridophenazine (dimerization constant = 289 ± 17 M^{-1}), di(pyridin2-yl)tetraazaphenazine (83 ± 17 M^{-1}) or tetraazatetrapyridopentacene, which reveal even stronger interactions between the extended π-systems of these ligands. [45,46,26,27,29] This might be important, because in case of high intermolecular association behavior self-quenching of excited states can get more favorable.[29,47-49]

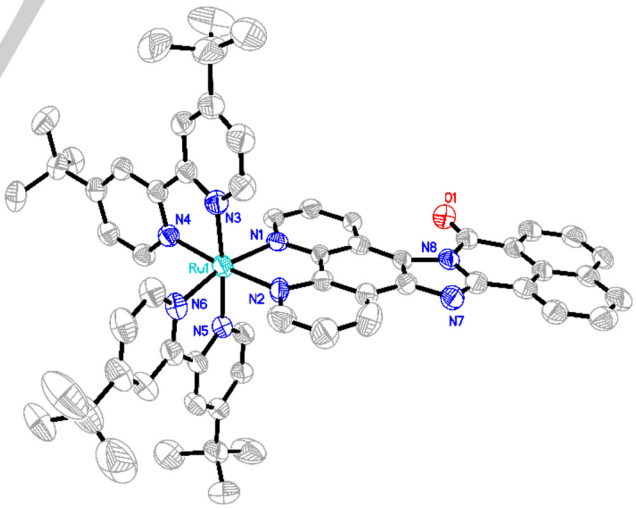

Figure 3. Solid-state structure (ORTEP representation) of **Rubiipo** with thermal ellipsoids at a probability level of 50%. Hydrogen atoms, PF_6^- counter anions and solvent molecules are omitted for clarity.

Single crystals of **Rubiipo** suitable for X-ray diffraction analysis were obtained by slow evaporation from a saturated acetonitrile/water mixture. **Rubiipo** crystallizes in the monoclinic space group C 2/c. Due to the asymmetric structure of **biipo**, two

enantiomers of **Rubiipo** are possible causing a geometrical disorder (see Figure S3.11) of the respective solid-state structure. Please note, that **Rubiipo** does not have different diastereomers, but exists as a mixture of enantiomers (Figure S3.13).[50] As clearly evident from the X-ray structural data, there are the expected enantiomers of the corresponding regioisomers of **Rubiipo** (Figure S3.13). In addition, the **biipo** ligand facilitates a certain degree of π-π interactions between the individual metal complex cations (Figure S3.12) similar to other extended rigid polyaromatic diimine ligands.[47,51] The obtained unit cell contains 8 Ru complexes along with 16 PF_6^- anions and 30 acetonitrile molecules. This resulted in a challenging crystal structure, where the second hexafluorophosphate anion is overlaid by several acetonitrile molecules. Interestingly, this obstacle and the need for several restraints was found in multiple measurements, but prevents a detailed discussion of exact bond lengths and angles. Nevertheless, with a final R-value of 6.4% the solid-state structure is still well suited to show the general properties, *e.g.* the conventional distorted octahedral type coordination environment around the ruthenium center[52] and the planar structure of **biipo**.

Electrochemical Properties

The redox properties of **Rubiipo** and **biipo** were studied by cyclic voltammetry and differential pulse voltammetry (Figure 4, Table 1) in acetonitrile solution containing 0.1 M $[Bu_4N][PF_6]$. The reversible Ru^{II}/Ru^{III} oxidation couple is located at 0.80 V *vs.* Fc/Fc^+, which is in accordance to related Ru(II) complexes, *e.g.* **Ruphen** (0.78 V) or **Rubpy** (0.89 V).[53,54]
The reversible reduction waves at -1.44, -1.86, -2.04 and -2.31 V are characteristic for $[(bpy)_2Ru(L)]^{2+}$ type complexes, where L represents a phen derivative with an extended π-system.[41,47] These potentials can be assigned to the stepwise reduction of (i) the naphthaloylene-benzene moiety of **biipo**, (ii)/(iii) the two tbbpy ligands and (iv) the phen part of the **biipo** ligand, respectively.[55,56] The first reduction event of **Rubiipo** (-1.44 V) is 150 mV shifted to more positive potentials compared to **biipo** (-1.59 V). This reduction is reversible for both compounds as also evidenced by scan-rate dependent CV measurements (Figure S5.2). This process can be attributed to the naphthaloylene-benzene moiety of **biipo**, which is supported by the DFT calculations of the reduced ligand, showing that the spin density is located at the backbone of the **biipo** ligand (Figure S8.2). However, the irreversible reduction process at -2.21 V of **Rubiipo** seems to be related to the imidazole unit as known from the literature.[41]

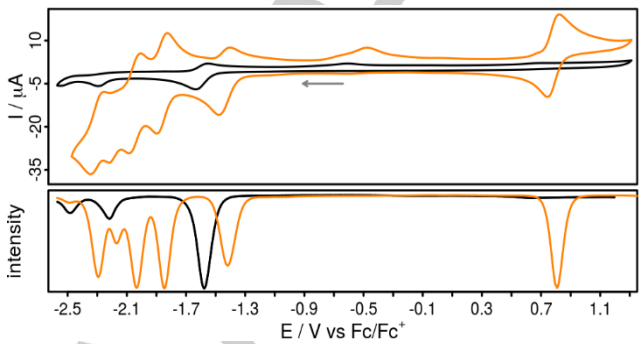

Figure 4. Cyclic voltammograms (top) and differential pulse voltammograms (DPV, bottom) of **biipo** (black, < 1 mM due to low solubility in acetonitrile) and **Rubiipo** (orange, 1 mM) in acetonitrile solution referenced *vs.* the ferrocene/ferricenium (Fc/Fc^+) couple. The current values of the DPV are normalized. Conditions: scan rate of 100 mVs^{-1}, $[Bu_4N][PF_6]$ (0.1 M) as supporting electrolyte.

Table 1. Summary of the photophysical and electrochemical properties of **biipo**, **Rubiipo** and of selected reference compounds in acetonitrile solution at room temperature. The electrochemical data were obtained from deaerated acetonitrile solutions at room temperature and are referenced vs. the ferrocene/ferricenium (Fc/Fc^+) couple.

Compound	$\lambda_{abs,max}$ [nm] (ε [10^3 M^{-1} cm^{-1}])	λ_{em} [nm] inert	φ_{em} inert	φ_{em} O_2	τ_{em} [ns] inert	τ_{em} [ns] O_2	$E_{1/2ox}$ [V]	$E_{1/2red}$ [V]
biipo	409 (6.2)	540	0.258	0.428	< 10 [b]	< 10 [b]	-	-1.59, -2.29[c]
phen[a]	265 (32.0)	365	< 0.01					
Rubiipo	411 (26.3), 460 (24.7)	623	0.022	0.006	1668, 24717	222	+ 0.80	-1.44, -1.86 -2.04, -2.21[c], -2.31
Ruphen[a]	426 (16), 455 (19)	602	0.03	-	272	-	+ 0.79	-1.79, -1.99, -2.26

[a] taken from reference 57; [b] the lifetime was below the detection limit; [c] irreversible redox event.

10.1002/chem.202001564

Absorption and Emission Properties

The **biipo** ligand absorbs in acetonitrile in a broad visible range up to 500 nm (Figure 5). This is a significant redshift compared to the **phen** ligand, which possesses an absorption maximum at around 365 nm.[57] The energetically lowest lying band could be assigned by TD-DFT calculations to a ligand centred (LC) π-π* transition from the phenanthroline/imidazole part to the naphthaloylenebenzene moiety of **biipo** (480nm, transition 1, Figure 5 and SI). At higher energies (*i.e.* the band at 350 nm) the situation is different and a transition from the naphthaloylenebenzene part to the phenanthroline unit occurs. These results indicate that although in the **biipo** ligand the naphthaloylenebenzene moiety is directly fused to the phenanthroline part, this ligand is still split into two separated halves concerning its orbitals in the ground and excited states. This results in a very broad absorption of the pure ligand.

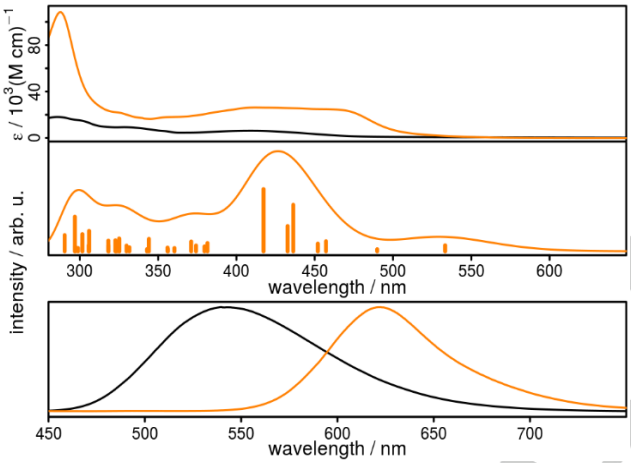

Figure 5. Spectra of **biipo** (black) and **Rubiipo** (orange). Top: UV/vis absorption spectrum in acetonitrile. Middle: Calculated absorption spectrum of **Rubiipo** resulting from the convolution (std. deviation 40) of the transitions above 290 nm (vertical bars) with a Gaussian function. The transition energies are calculated at full TD-DFT level of theory (B3LYP-D3(BJ)/def2-TZVP. Bottom: Emission spectra in acetonitrile under oxygen free conditions.

In comparison to **Ruphen**,[57] having an absorption maximum at 444 nm in the metal-to-ligand charge transfer (MLCT) transition, **Rubiipo** possesses a broader MLCT band with two maxima located at 411 and 460 nm, respectively. This latter prominent feature can be explained by MLCT transitions from the ruthenium centre to the two tbbpy ligands and to the phen part of **biipo** (Table S9.2) Additionally, the MLCT transition with the lowest energy ends also directly at the naphthaloylenebenzene moiety (c.f. inset of Figure 6, SI) as supported by TDDFT calculations. However, in the calculations the LC π-π* transitions of **Rubiipo** are redshifted from 320 nm to 370 nm compared to the transitions of the uncoordinated **biipo** ligand. Contrary, the π-π* transition to the naphthaloylenebenzene moiety is clearly blueshifted from 480 nm (**biipo**) to 417 nm (**Rubiipo,** transition 12, Table S9.2). For these reasons, the absorption maximum at around 411 nm is very intense causing the high attenuation coefficient of **Rubiipo** in this region of the absorption spectrum. Nevertheless, above 420 nm the MLCT transitions in **Rubiipo** are not overlaid by the LC transitions, which is commonly observed for related systems containing diimine ligands with an extended π-system.[41,49,58-60] There, the MLCT transitions are often superimposed by the LC transitions.[41,49]

The emission properties of **biipo** and **Rubiipo** differ significantly from each other. The ligand emits at about 540 nm and is almost unaffected by the presence of oxygen in the acetonitrile solution (Figure 5 bottom). In strong contrast, **Rubiipo** is almost non-emissive under aerated conditions, but exhibits a clear emission at 623 nm in the absence of oxygen with a quantum yield of about 2.2% (Table 1). This quantum yield is in the same order of magnitude as some related Ru(II) complexes,[52] but lower than a heteroleptic Ru(II) complex with an azabenz-annulated perylene bisimide (11%).[28] Remarkably, the emission intensity is drastically reduced already by small traces of oxygen. Thus, **Rubiipo** is highly sensitive vs. oxygen and a good oxygen sensor due to the strong quenching of emission.[61]

In accordance to the steady state emission measurements the emission lifetimes of **Rubiipo** were also determined in acetonitrile (Figure 6). Under aerated conditions a lifetime of 222 ns was obtained (Figure S6.1), which is comparable to the related complex $[(bpy)_2Ru(PNI\text{-}phen)]^{2+}$ (with PNI = 4-piperidinyl-1,8-naphthalimide), where the π extension is not directly fused to the phenanthroline part.[25] Under inert conditions the emissive excited state lives remarkably longer (Figure 6). Analysis of the kinetics revealed a biexponential decay with two time constants of τ_1 = 1.7 µs and τ_2 = 24.7 µs, which belong to LC or MLCT transitions. Thus, **Rubiipo** emits about 100 times longer when changing from ambient to oxygen free conditions. This is again comparable to $[(bpy)_2Ru(PNI\text{-}phen)]^{2+}$ with a lifetime of 27.6 µs under inert conditions. Nevertheless, to the best of our knowledge this is a large increase in excited state lifetime for such a Ru(II) complex containing a diimine ligand with a fully conjugated and extended π-system. Interestingly, the second time constant is highly oxygen sensitive. As soon as **Rubiipo** gets in contact with O_2 τ_2 considerably decreases to only sub microseconds. This again underlines the strong oxygen sensitivity of **Rubiipo**.

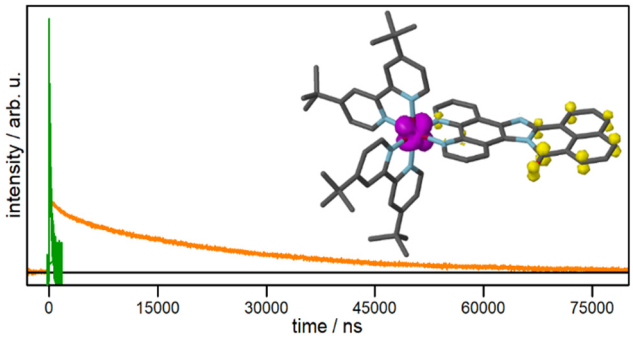

Figure 6. Emission lifetime of **Rubiipo** in acetonitrile under ambient (green) and inert conditions (orange). The respective fits and the residuals are depicted in the SI. The inset (differential density plot of **Rubiipo**) shows one of the occurring MLCT transitions from the Ru d orbital to the π* orbital located at the naphthaloylenebenzene moiety.

10.1002/chem.202001564

Transient Absorption Spectroscopy

To verify the obtained excited state lifetimes by a different method time-resolved transient absorption spectroscopy was performed. Under inert conditions and excited at 355 nm, a very broad excited state absorption from 480 to 700 nm was obtained for **Rubiipo** in acetonitrile solution (Figure 7). This is a typical observation, if ligand-centred transitions are detected by transient absorption spectroscopy.[60,62] Due to this feature the expected ground state bleach was only extended up to 440 nm and not up to 500 nm, as estimated from the steady state absorption spectra (Figure 5 top). The kinetics (Figure 7) were analysed globally over the whole range from 370 to 700 nm by a biexponentially fit function. The received lifetimes τ_1 = 2.5 and τ_2 = 24.9 µs are comparable to the ones obtained for the emission lifetime under oxygen-free conditions. It should be noted, that especially the longer lifetime is very oxygen sensitive. As soon as there are traces of oxygen present, this time constant decreases significantly. Thus, it is very important to work under fully inert conditions for the determination of the excited state lifetimes of **Rubiipo**. Under aerobe conditions the monoexponential fit of the data results in one time constant, *i.e.* τ = 261 ns, which is also comparable to the obtained emission lifetimes in the presence of oxygen.

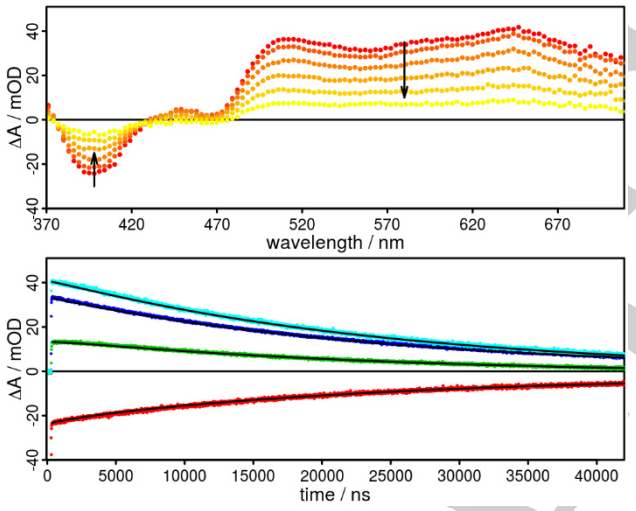

Figure 7. Transient absorption spectra (top) from 500 (red) to 40000 ns (yellow)and respective kinetics (bottom) of **Rubiipo** in acetonitrile excited at 355 nm under inert conditions. Kinetics at 390 (red), 480 (green), 500 (blue) and 650 nm (light blue), the black line belongs to the fits with two time constants of 2.5 and 24.9 µs.

Oxygen sensitivity and productivity

Motivated by the strong oxygen sensitivity **Rubiipo** was tested for its ability to produce singlet oxygen upon light irradiation. $^1O_2$ is the leading actor in Type II pathway of Photodynamic Therapy (PDT) actions. An efficient production of reactive singlet oxygen under oxygen containing conditions is still a crucial point for this type of application.[5,63] To verify the $^1O_2$ production by **Rubiipo**, a solution of ABDA (9,10-anthracenediyl-bis(methylene)dimalonic acid) in PBS (phosphate buffered solution) was added to distinct quantities (c = 1 µM) of **Rubiipo**, **Rubpy** and **Ruphen** (ABDA:Ru = 50:1), respectively. ABDA is a commonly applied singlet oxygen detection agent, due to its very selective reaction with this reactive oxygen species (ROS). $^1O_2$ and ABDA build up an endoperoxide (Figure S4.5), which loses the characteristic anthracene absorption bands at around 350 to 410 nm.[64-66] Upon irradiation with blue light (LED, 470 nm, 50 mWcm^{-2}) under constant cooling **Rubiipo** (Figure 8 top) shows very fast depletion of the ABDA absorbance at around 360, 380 and 400 nm. In order to evaluate the singlet oxygen productivity, the decrease of this absorption band was plotted against time until complete consumption of ABDA (Figure 8 bottom). The observed decay was not linearly, but seemed to be an exponential decrease, which is much faster compared to **Ruphen** (Figure 8 bottom). Whereas also **Rubpy** evolves $^1O_2$ much slower compared to **Rubiipo** (Figures S4.6-S4.10). Nevertheless, a better energy transfer rate from **Rubiipo** to oxygen can neither be assessed nor excluded based on the current data and further investigations concerning this issue are needed.

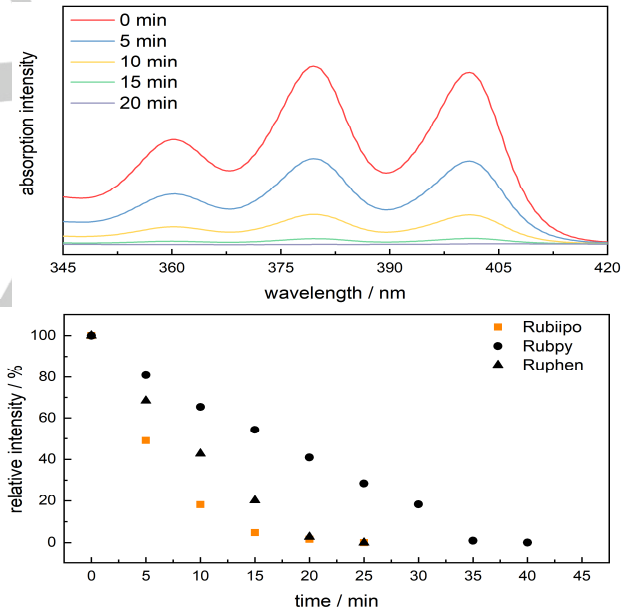

Figure 8. Top: Singlet oxygen evolution experiment using **Rubiipo** (1 eq.) and ABDA (50 eq.) in PBS after irradiation with blue light (50 mWcm^{-2}, 470 nm) in the range of ABDA absorbance (se also Figure S4.5.). Bottom: Comparison of the relative ABDA absorbance as function of time during irradiation of **Rubiipo** (squares), **Rubpy** (circles) and **Ruphen** (triangles) with blue light (50 mWcm^{-2}, 470 nm). It becomes clear, that **Rubiipo** degrades ABDA the fastest. See for the specific ABDA test in the SI the section 4.

Conclusions

In summary, starting from 1,10-phenanthroline a new type of a polycyclic, fully conjugated and rigid diimine ligand with a

naphthaloylenebenzene moiety in the back was prepared for the first time. Based on the special ligand structure, a Ru(II) photosensitizer (**Rubiipo**), also verified by single crystal X-ray diffraction analysis, with some unique properties was formed. For instance, **Rubiipo** shows a reversible redox chemistry (*i.e*. four reductions and one oxidation) as well as a strong and broad absorption in the visible with two maxima at 411 and 460 nm, respectively. More importantly, **Rubiipo** possesses a clear emission at 623 nm with very long-lived excited states of 1.7 and 24.7 µs in acetonitrile in the absence of oxygen. Interestingly, the emission intensity and lifetimes are drastically decreased (by a factor of >100) by O_2, which indicates a high oxygen sensitivity of this complex. In the future, temperature-dependent emission, emission lifetime and spectroelectrochemical measurements are planned, to clarify the nature of the excited states further. In addition, a detailed investigation of the oxygen sensing ability of **Rubiipo** will be assessed by Stern-Volmer quenching experiments.

Most importantly, beside potential applications as an oxygen sensor **Rubiipo** is able to produce singlet oxygen under visible light irradiation with very fast kinetics. Therefore, the study of further applications of the **Rubiipo** photosensitizer as well as of other transition metal complexes using the new **biipo** ligand are currently ongoing.

Experimental Section

CCDC 1993565 (**Rubiipo**) contains the supplementary crystallographic data for this paper. This data is provided free of charge by The Cambridge Crystallographic Data Centre.

For further details see the Supporting information: Experimental and synthetic details, further crystallographic data, NMR, MS, IR, UV/vis, and emission spectra, photostability measurements, singlet oxygen evolution measurements, cyclic voltammograms, emission lifetime analysis, transient absorption spectra, TD-DFT calculation data.

Acknowledgements

Y.Y., M.K. and S.T. grateful acknowledge the German Science Foundation (DFG, Priority Program SPP 2102 “Light-controlled reactivity of metal complexes” (KA 4671/2-1 and TS 330/4-1) and the DFG project TS 330/3-1) for funding. S.R. is thankful for financial support from the DFG within the collaborative research center TRR 234 Catalight. J.B. gratefully acknowledges the Fonds der Chemischen Industrie (FCI) for a Kekulé-Stipendium. The authors acknowledge support by the state of Baden-Württemberg through bwHPC and by the DFG (INST 40/467-1 FUGG). The authors also thank Bernd Maier, Martin Rentschler and Julian Bösking for their synthetic work and Dr. Dieter Sorsche for providing X-ray data.

Keywords: ruthenium photosensitizer • extended π-system • electron storage • excited state properties • singlet oxygen evolution

[1] M. H. Shaw, J. Twilton, D. W. C. MacMillan *J. Org. Chem.* **2016***, 81 (16),* 6898–6926.
[2] S. Malzkuhn, O. S. Wenger *Coord. Chem. Rev.* **2018***, 359*52–56.
[3] Q. M. Kainz, C. D. Matier, A. Bartoszewicz, S. L. Zultanski, J. C. Peters, G. C. Fu *Science* **2016***, 351 (6274),* 681.
[4] J. Twilton, C. C. Le, P. Zhang, M. H. Shaw, R. W. Evans, D. W. C. MacMillan *Nat. Rev. Chem.* **2017***, 1 (7),* 0052.
[5] R. Eisenberg *Science* **2009***, 324 (5923),* 44.
[6] P. D. Frischmann, K. Mahata, F. Würthner *Chem. Soc. Rev.* **2013***, 42 (4),* 1847–1870.
[7] S. Berardi, S. Drouet, L. Francàs, C. Gimbert-Suriñach, M. Guttentag, C. Richmond, T. Stoll, A. Llobet *Chem. Soc. Rev.* **2014***, 43 (22),* 7501–7519.
[8] Y.-J. Yuan, Z.-T. Yu, D.-Q. Chen, Z.-G. Zou *Chem. Soc. Rev.* **2017***, 46 (3),* 603–631.
[9] T. J. Dougherty, C. J. Gomer, B. W. Henderson, G. Jori, D. Kessel, M. Korbelik, J. Moan, Q. Peng *J. Natl. Cancer Inst.* **1998***, 90 (12),* 889–905.
[10] P. R. Ogilby *Chem. Soc. Rev.* **2010***, 39 (8),* 3181–3209.
[11] D. Van Straten, V. Mashayekhi, S. H. De Bruijn, S. Oliveira, J. D. Robinson *Cancers* **2017***, 9 (2),*
[12] S. Monro, K. L. Colón, H. Yin, J. Roque, P. Konda, S. Gujar, R. P. Thummel, L. Lilge, C. G. Cameron, S. A. McFarland *Chem. Rev.* **2019***, 119 (2),* 797–828.
[13] M. C. DeRosa, R. J. Crutchley *Coord. Chem. Rev.* **2002***, 233-234*351–371.
[14] C. Mari, V. Pierroz, S. Ferrari, G. Gasser *Chem. Sci.* **2015***, 6 (5),* 2660–2686.
[15] G. Shi, S. Monro, R. Hennigar, J. Colpitts, J. Fong, K. Kasimova, H. Yin, R. DeCoste, C. Spencer, L. Chamberlain, A. Mandel, L. Lilge, S. A. McFarland *Coord. Chem. Rev.* **2015**, *282-283*, 127-138.
[16] F. Heinemann, J. Karges, G. Gasser *Acc. Chem. Res.* **2017***, 50 (11),* 2727–2736.
[17] R. Konduri, N. R. de Tacconi, K. Rajeshwar, F. M. MacDonnell *J. Am. Chem. Soc.* **2004***, 126 (37),* 11621–11629.
[18] S. Singh, N. R. de Tacconi, N. R. G. Diaz, R. O. Lezna, J. Muñoz Zuñiga, K. Abayan, F. M. MacDonnell *Inorg. Chem.* **2011***, 50 (19),* 9318–9328.
[19] S. Karlsson, J. Boixel, Y. Pellegrin, E. Blart, H.-C. Becker, F. Odobel, L. Hammarström *Faraday Discuss.* **2012***, 155 (0),* 233–252.
[20] J. M. Aslan, D. J. Boston, F. M. MacDonnell *Chem. Eur. J.* **2015***, 21 (48),* 17314–17323.
[21] L. Hammarström *Acc. Chem. Res.* **2015***, 48 (3),* 840–850.
[22] Y. Zhang, P. Traber, L. Zedler, S. Kupfer, S. Gräfe, M. Schulz, W. Frey, M. Karnahl, B. Dietzek *Phys. Chem. Chem. Phys.* **2018***, 20 (38),* 24843–24857.
[23] E. H. Yonemoto, R. L. Riley, Y. I. Kim, S. J. Atherton, R. H. Schmehl, T. E. Mallouk *J. Am. Chem. Soc.* **1992***, 114 (21),* 8081–8087.
[24] A. Lavie-Cambot, C. Lincheneau, M. Cantuel, Y. Leydet, N. D. McClenaghan *Chem. Soc. Rev.* **2010***, 39 (2),* 506–515.
[25] D. S. Tyson, C. R. Luman, X. Zhou, F. N. Castellano *Inorg. Chem.* **2001***, 40 (16),* 4063–4071.
[26] D. E. Polyansky, E. O. Danilov, F. N. Castellano *Inorg. Chem.* **2006***, 45 (6),* 2370–2372.
[27] J. Hankache, O. S. Wenger *Phys. Chem. Chem. Phys.* **2012***, 14 (8),* 2685–2692.
[28] M. Schulze, A. Steffen, F. Würthner *Angew. Chem. Int. Ed.* **2015**, *54*, 1570-1573.
[29] H. Langhals *Heterocycles* **1995***, 40 (1),* 477–500.
[30] A. Hermann, K. Müllen *Chem. Lett.* **2006**, *35 (9)*, 978-985.
[31] T. Weil, T. Vosch, J. Hofkens, K. Peneva, K. Müllen *Angew. Chem. Int. Ed.* **2010**, *49 (48)*, 9068-9093.

[32] M. Pan, X.-M. Lin, G.-B. Li, C.-Y. Su *Coord. Chem. Rev.* **2011***, 255 (15),* 1921–1936.
[33] F. N. Castellano *Dalton Trans.* **2012***, 41 (28),* 8493–8501.
[34] S.-L. Suraru, F. Würthner *Angew. Chem. Int. Ed.* **2014***, 53 (29),* 7428–7448.
[35] F. Würthner, C. R. Saha-Möller, B. Fimmel, S. Ogi, P. Leowanawat, D. Schmidt Chem. Rev. **2016**, *116 (2)*, 962-1052.
[36] H. Langhals, H. Jaschke *Chemistry - A European Journal* **2006***, 12 (10),* 2815–2824.
[37] Z. Yuan, Y. Xiao, Z. Li, X. Qian *Org. Lett.* **2009***, 11 (13),* 2808–2811.
[38] M. Mamada, C. Pérez-Bolívar, D. Kumaki, N. A. Esipenko, S. Tokito, P. Anzenbacher Jr. *Chem. Eur. J.* **2014***, 20 (37),* 11835–11846.
[39] M. Karnahl, S. Tschierlei, C. Kuhnt, B. Dietzek, M. Schmitt, J. Popp, M. Schwalbe, S. Krieck, H. Görls, F. W. Heinemann, S. Rau *Dalton Trans.* **2010***, 39 (9),* 2359–2370.
[40] H. Yin, M. Stephenson, J. Gibson, E. Sampson, G. Shi, T. Sainuddin, S. Monro, S. A. McFarland *Inorg. Chem.* **2014***, 53 (9),* 4548–4559.
[41] D. Isakov, R. Giereth, D. Nauroozi, S. Tschierlei, S. Rau *Inorg. Chem.* **2019***, 58 (19),* 12646–12653.
[42] M. Skaisgirski, X. Guo, O. S. Wenger *Inorg. Chem.* **2017***, 56 (5),* 2432–2439.
[43] V. Steullet, D. W. Dixon *J. Chem. Soc., Perkin Trans. 2* **1999** *(7),* 1547–1558.
[44] de Tacconi, R. Norma, R. Chitakunye, F. M. MacDonnell, R. O. Lezna *J. Phys. Chem. A* **2008***, 112 (3),* 497–507.
[45] M. G. Pfeffer, C. Pehlken, R. Staehle, D. Sorsche, C. Streb, S. Rau *Dalton Trans.* **2014***, 43 (35),* 13307–13315.
[46] F. Huber, D. Nauroozi, A. K. Mengele, S. Rau *Eur. J. Inorg. Chem.* **2017**, 4020-4027.
[47] J. Bolger, A. Gourdon, E. Ishow, J.-P. Launay *Inorg. Chem.* **1996***, 35 (10),* 2937–2944.
[48] S. D. Bergman, M. Kol *Inorg. Chem.* **2005***, 44 (6),* 1647–1654.
[49] L. Troian-Gautier, C. Moucheron *Molecules (Basel, Switzerland)* **2014***, 19 (24759069),* 5028–5087.
[50] L. Gong, M. Wenzel, E. Meggers *Acc. Chem. Res*. **2013**, *46 (11)*, 2635–2644.
[51] M. Karnahl, C. Kuhnt, F. W. Heinemann, M. Schmitt, S. Rau, J. Popp, B. Dietzek *Chem. Phys.* **2012**, *393*, 65-73.
[52] A. Juris, V. Balzani, F. Barigelletti, S. Campagna, P. Belser, A. von Zelewsky *Coord. Chem. Rev.* **1988***, 84*85–277.
[53] S. Rau, R. Fischer, M. Jäger, B. Schäfer, S. Meyer, G. Kreisel, H. Görls, M. Rudolf, W. Henry, J. Vos *Eur. J. Inorg. Chem.* **2004***,* 2001–2003.
[54] L. A. Büldt, A. Prescimone, M. Neuburger, O. S. Wenger *Eur. J. Inorg. Chem.* **2015**, 4666–4677.
[55] P. Wintergerst, A. K. Mengele, D. Nauroozi, S. Tschierlei, S. Rau *Eur. J. Inorg. Chem.* **2019***,* 1988–1992.
[56] S.-H. Fan, A.-G. Zhang, C.-C. Ju, L.-H. Gao, K.-Z. Wang *Inorg. Chem.* **2010***, 49 (8),* 3752–3763.
[57] M. Karnahl, S. Krieck, H. Görls, S. Tschierlei, M. Schmitt, J. Popp, D. Chartrand, G. S. Hanan, R. Groarke, J. G. Vos, S. Rau *Eur. J. Inorg. Chem.* **2009***,* 4962–4971.
[58] R. Giereth, I. Reim, W. Frey, H. Junge, S. Tschierlei, M. Karnahl *Sustainable Energy Fuels* **2019**, *3*, 692-700.
[59] Y Sun, L. E. Joyce, N. M. Dickson, C. Turro *Chem. Commun.* **2010**, *46*, 2426-2428.
[60] J. Schindler, Y. Zhang, P. Traber, J.-F. Lefebvre, S. Kupfer, M. Demeunynck, S. Gräfe, M. Chavarot-Kerlidou, B. Dietzek *J. Phys. Chem. C* **2018**, *122 (1)*, 83-95.
[61] J. N. Demas, B. A. DeGraff, P. B. Coleman *Anal. Chem.* **1999***, 71 (23),* 793A–800A.
[62] D. S. Tyson, K. B. Henbest, J. Bialecki, F. N. Castellano *J. Phys. Chem. A* **2001**, *105 (35)*, 8154-8161.
[63] K. Plaetzer, B. Krammer, J. Berlanda, F. Berr, T. Kiesslich *Lasers Med. Sci.* **2009***, 24 (2),* 259–268.
[64] T. Wang, N. Zabarska, Y. Wu, M. Lamla, S. Fischer, K. Monczak, D. Y. W. Ng, S. Rau, T. Weil *Chem. Commun.* **2015***, 51 (63),* 12552–12555.
[65] O. Planas, N. Macia, M. Agut, S. Nonell, B. Heyne *J. Am. Chem. Soc.* **2016***, 138 (8),* 2762–2768.
[66] S. Chakrabortty, B. K. Agrawalla, A. Stumper, N. M. Vegi, S. Fischer, C. Reichardt, M. Kögler, B. Dietzek, M. Feuring-Buske, C. Buske, S. Rau, T. Weil *J. Am. Chem. Soc.* **2017***, 139 (6),* 2512–2519.

10.1002/chem.202001564

WILEY-VCH

FULL PAPER

Entry for the Table of Contents

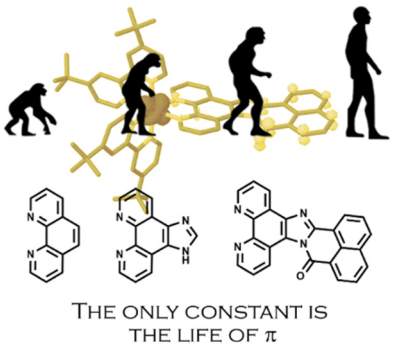

The constant evolution of phenanthroline leads to a new type of a polycyclic, fully conjugated and rigid diimine ligand with a naphthaloylenebenzene moiety in the back. The so-called biipo ligand enabled a Ru(II) photosensitizer, which has an excited state lifetime of up to 24.7 µs and is active for the light-driven singlet oxygen production.